

# Influence Of intake Scenarios On heat transfer performance of hydrogen fueled Engine

Soni Kumari

Department of Mechanical Engineering, GLA University, Mathura 281406, India

## Abstract-

This research utilized steady state simulation to explore the impact of input charge inlet conditions on in-cylinder heat transfer characteristics for the port injection Gasoline hydrogen Fueled Engine H2ICE. The governing equations of the engine designer's elements are defined by the one-dimensional gas structure. First the governing equations were inserted and the model description was presented briefly. Measure increasing rpm and AFR, as well as the impact of changing input charges parameters (force and temp). The speed of the motor was changed in 1000-rpm increments from 2100 to 5000 rpm, and the AFR was changed from particle surface to light limit. The inlet pressure was varied in 0.05-bar increments between 0.95 and 1.05 bar, and the temperature range was ranged in 10-degree increments between 270 and 320 degrees. The results indicate that the impact of infusion liquid phase, AFR, and max torque through the in-heat transfer performance for piston insertion H2ICE are discussed within the work. Variations in intake pressure have a greater effect on heat transfer characteristics than temperature variations, according to the results. This was also revealed why changing the intake charge pressure had little effect on lean mixtures. Furthermore, the obtained results are supported by an examination of the in-cylinder rate transfer of heat relationship in rotational speeds.

**Keywords:** Thermal conductivity, gasoline engine, intake conditions, pump infusion, energy transfer.

## Introduction

Transportation's energy usage is increasingly increasing as a result of advances in the industrial world, where new technologies are implemented on a daily basis. Petroleum reserves are rapidly depleting, and air quality is deteriorating, raising concerns about the future. Since crude oil supplies are finite, the production of alternative fuel engines has piqued the interest of the engine community. Alternative fuels are useful in helping to mitigate fuel shortages and reduce engine exhaust emissions (Huang et al. 2006; Saravanan et al. 2007). The tests showed better input charge pressure, with varying motor speed and AFR, have a detrimental effect on the interface cylinder heat transfer coefficient. If the AFR increases, the temperature of the intake charge does not affect the rate of heat transfer for the in-cylinder, and when the engine speed changes it has a slight effect. Variations in intake pressure have a greater effect on heat transfer characteristics than temperature variations, according to the results. This was also revealed why changing the intake charge pressure had little effect on lean mixtures. One of several alternative sources of energy is hydrogen. As a renewable fuel, hydrogen has unique properties that give it a superior impact over other fuels. Hydrogen is a green alternative to fossil fuels that has the ability to build environmentally friendly mobility systems when used as a vehicle fuel. Internal combustion engines that run on hydrogen have been the focus of a lot of research. In response to increasing worries about resource depletion and pollution prevention, authors have built a gas generator that can use a variety of fuel delivery methods (Eichseder, et al. 2003; Kim, et al. 2005; Ganesh, et al. 2008). The intake charge conditions have long been known to affect an engine's output. The purpose of this research is to find out how effective air intake charges parameters (temperature and pressure) are at reducing in-cylinder thermal performance in pump insertion H2ICE. The correlation's initial constant values were compounded by 1.8, yielding a better fit with the research observations (Aceves and Smith, 1997). The authors discovered that the heat transfer relationship underpredicts thermal energy depletion during the research. The intake pressure and temperature are the two most significant intake conditions that affect gas engine output (Soares and Sodre, 2002; Sodre and Soares, 2003). The purpose of this research is to find out how effective air intake charges parameters (temperature and pressure) are at reducing in-cylinder thermal performance in pump insertion H2ICE.

## Materials and Methods

Using the GT suite programme, A solitary fuel cell model with port insertion was established. It was looked into injecting hydrogen into the intake port in the centre. A theoretical model of a solitary fuel cell engine is shown in Figure 1. The engine specifications used to build the model are mentioned in Table 1. (A). The inlet and outlet ports of the engine cylinders are symmetrically patterned by gas tubes using a ring attachment. The flow dimensions of the orifice of the bell were standardized to 1. The inlet rod is connected to the inlet runners with a diameter of 0.05 meters and a length of 0.099 m. The fuel system and drywall pistons have a larger volume than this. The heat generator was used to reward the valve and stem bends, additional surface area and turbulence. The pressure drop was included in the coefficients of valve discharge but no additional pressure drop was included for surface rugging. A rounded pipe with a diameter of 0.04 m and a length of 0.8 m was used to model the exhaust port. A model embedded in each drain was used to determine the temperature of the exhaust wall. A visualization of both the surface energy transfer is needed for an accurate analysis of the ICE working process. The generator method incorporates Woschni's correlation for the in heat transfer calculation (Woschni, 1967). The effect of intake charge conditions on in-cylinder heat transfer, on the other hand, is poorly understood. The purpose of this research is to find out how effective air intake charges parameters (temperature and pressure) are at reducing in-cylinder thermal performance in pump insertion H2ICE. The

correlation's initial constant values were compounded by 1.8, yielding a better fit with the research observations (Aceves and Smith, 1997). The authors discovered that the heat transfer relationship underpredicts thermal energy depletion during the research.

**Table 1:** Engine specifications for model A.

| Unit      | Value | Parameter             |
|-----------|-------|-----------------------|
| -         | 3     | No. of Cylinder       |
| CA (ATDC) | 40    | Exhaust Valve Close   |
| CA (ABDC) | 87    | Inlet Valve Close     |
| CA (BBDC) | 58    | Exhaust Valve Open    |
| CA (BTDC) | 10    | Inlet Valve Open      |
| -         | 10.5  | Compression Ratio     |
| mm        | 222   | Connecting Rod Length |
| mm        | 105   | Stroke                |
| mm        | 105   | Bore                  |

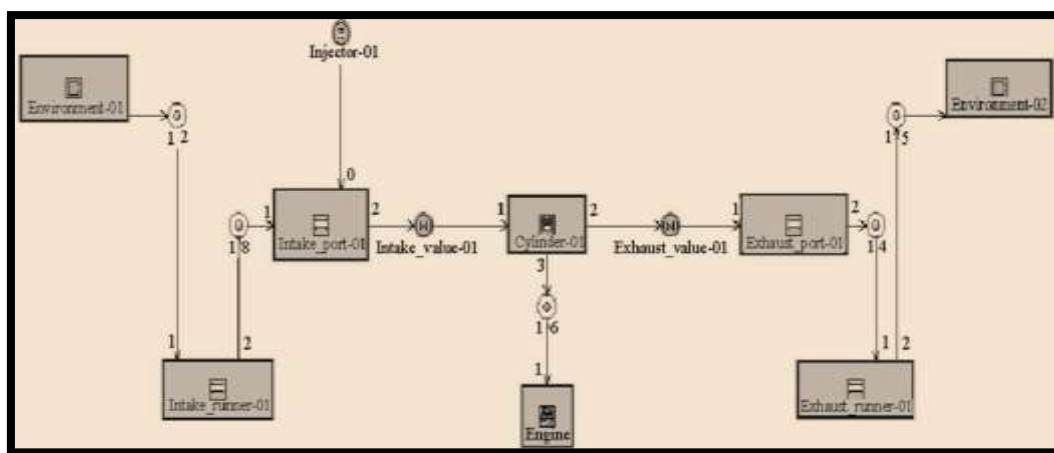


**Figure 1:** A solitary, multiple strokes, hydrogen-fuelled engine with pump insertion.

### Equations for Heat Exchange Simulation

The rate of heat transfer of the fuel models is described by using a single dimensional gas dynamic model to make up for bends, additional surface area and valve and stem turbulence. Pressure drop includes a valve discharge coefficient but no surface roughness additional pressure loss is used. A rounded pipe with a diameter of 0.04 m and a length of 0.8 m was used to model the exhaust port. A model embedded in each drain was used to determine the temperature of the exhaust wall. To assess engine performance, researchers will look at the weight, movement, and flow of energy between specific mechanical parts, as well as the energy and working transfers within each part. In the simulation model, other formulas are used in addition to the main wave equation to determine the temperature pressure loss, coefficient of friction, and temperature distribution.

The pressure drops equation is solved as follows:

$$C_{pl} = \frac{p_1 - p_2}{\frac{1}{2} \rho v_1^2} \quad (1)$$

where  $p_1$  and  $p_2$  denote the suction and discharge pressures,  $\rho$  surface charge density and  $v$  inlet velocity respectively. Equation (2) and (3) can be used to express the friction coefficient for laminar and turbulent flow walls, respectively:

$$C_f = \frac{16}{Re_D} \quad Re_D < 2000; \quad Re_D = \frac{vD}{\nu}$$

$$C_f = \frac{0.08}{Re_D^{0.25}} \quad Re_D > 4000 \quad (2)$$

$$C_{f(rough)} = \frac{0.25}{(2 \log_{10}(\frac{D}{z})) + 1.74} \quad (3)$$

Reynolds number, diameter of pipe, and roughness height are all represented by  $Re_D$ ,  $D$ , and  $z$ , respectively. In the simulation model, other formulas are used in addition to the main wave equation to determine the temperature pressure loss, coefficient of friction, and temperature distribution.

The sum of thermal energy from the exhaust gasses inside the container to its boundaries is calculated using Newton's theory of cooled formula:

$$Aaaa(T_g - T_w) \quad (4)$$

A,a, Tg, and Tw are the heat exchange quantity, heat exchange region, gas temperature, and wall temperature, respectively.

The heat transfer coefficient is affected by the duration of the characteristic, the transport properties, the friction, the temperature, and the characteristic velocity. Eichelberg's equation (Eichelberg 1939), Woschni's equation (Woschni 1967), and Annand's equation are only a few of the heat transfer correlations that can be used to describe the heat transfer process within a combustion chamber (Annand 1963). The engine specifications used to build the model are mentioned in Table 1. (A). The intake and exhaust ports of the engine cylinder are modelled symmetrically including tubes, to gas entering the pipe across a ring appendage. The flow parameters of the bell mouth orifice became normalised to 1 ensure a smooth transition. A method that imitates the standard Woschni connection is used to calculate thermal performance inside the container. Unlike most of the other comparisons, Woschni divided the flow rates into two components: the unloaded gas velocity, which would be simply the ratio piston frequency, and the moment, combustion-induced velocity distribution. Equation (5) can be used to calculate the temperature distribution:

$$h = 3.26D^{-0.2}P^{0.8}T_g^{-0.55}w^{0.8}$$

$$w = 2.28C_m + 0.00334 \frac{(P-P_m)V_h T_r}{P_r V_r} \quad (5)$$

where D, P, Pm, Tg, V, Cm, Vh and r are the terms included to identify the volume, the average piston speed, and reference currency angle are boring diameter, pressure, engine pressure, gas temperature, volume, mean hydraulic speed and source curb angle. This system holds a constant velocity all throughout artillery shell portion of the process before introducing a steep velocity rise until combustion pressure reaches motoring force. This mathematical formula for natural gas electric motors was developed using the turbulent thermal efficiency process for cylinders. A practical approximation of the wall energy transfer is required for an interesting description of the ICE production line. As a consequence, the equation that offers the best approximation for the level of heat transfer from the fuel tank for fuel cell engine used. The effective in driving for (Aceves and Smith 1997) calculates engine temperature difference using Woschni's relation (Woschni 1967). It was revealed during the research that the heat exchange relationship underpredicts heat transfer loss. As an effect, for the previous arrangement, the initial values of the variables in the relationship were compounded by 1.8, leading to an improved match with the empirical observations.

### Results and Discussion

Stable state fuel convective heat transfer calculations of a four - cylinder ports injection liquid propellant gasoline fuelled engine are working with the effect of variation of injection pressure (temperatures and pressures) for two process parameter, Engine rpm and the Air-Fuel Ratio (AFR). In comparison, at 0.05 intervals, the inlet and outlet varied from 0.96 bar to 1.06 bar, and the pressure drop ranged from 280 to 320 degree.

### Affirmation of the Design

The original validation of this thesis was based on the findings of (Lee et al., 1995). Table 2 lists the platform specs from (Lee et al., 1995), as well as the latest single cylinder port inject engine model (B). For this testing, the same model configuration as in Figure 1 was used. To fit Lee et al findings, the engine and AFR were set to 1600 rpm and 68.66, respectively, in this comparison. The in-cylinder pressure traces for the base method (B) and laboratory experiments documented results are shown in Figure 2. (Lee et al., 1995). The thermal conductivity has improved with rising engine speed due to increased main driver (forced convection) with energy transfer inside the cylinder. Steadily increasing AFR lowers the energy content of the hydraulic cylinder air intake charge, thus declining AFR raises the energy density of the crank shaft air intake charge. The in-cylinder pressure track has a fair fit during compression stroke and acceptable patterns during heating process, but the out-of-cylinder pressure trace does not. Apart from the differences between certain engine specification requirements not specified in the report, due to the difficulty in ignition, as reported by Lee et al (Lee et al., 1995). Despite the designer's contradictions, the present model (B) and research data provide a high level of consensus. Figure 3 compares the approved model (A) to model (B) in terms of in-cylinder stress traces to demonstrate the embraced model's effectiveness for the present study. These variations account for changes in proportions and maintain its current between both the designs.

**Table 2:** Design parameters for the cylinders.

| Engine parameter      | Lee et al. (1995) | Present Model B |
|-----------------------|-------------------|-----------------|
| Bore                  | 86                | 86              |
| Stroke                | 87                | 87              |
| TDC Clearance height  | NA*               | 4               |
| Piston pin offset     | NA                | 2               |
| Connecting rod length | NA                | 151             |
| Compression ratio     | 8.6               | 8.7             |
| Inlet valve open      | 17                | 17              |
| Exhaust valve open    | 53                | 53              |
| Inlet valve close     | 55                | 55              |
| Exhaust valve close   | 13                | 13              |

\* NA=not available.

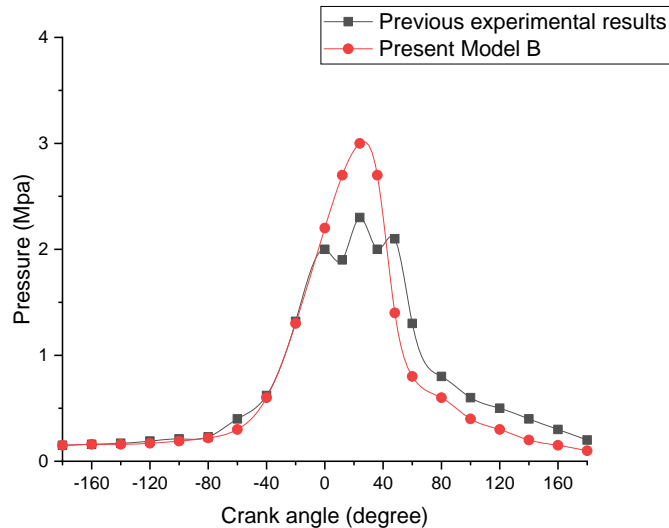


**Figure 2:** Results are compared of research observations reported by Lee et al. (1995) with the recent single port infusion engine system based on in-cylinder pressure residues.

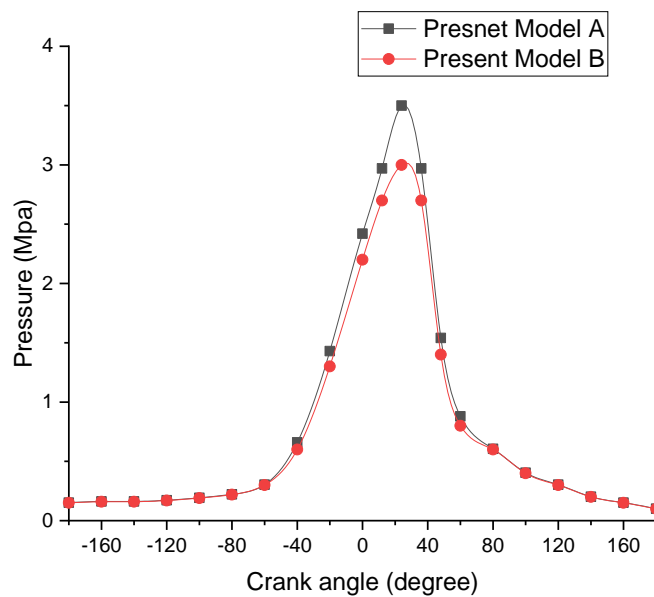


**Figure 3** On the basis of in-cylinder pressure residues, a distinction among designs (A and B)

### Injection Charge Pressure's Impact on Heat Transfer Rate

At different engine loads, figure 4 illustrates the influence of inlet and outlet through in heat transfer rate. The in-cylinder velocity and temperature rise as the input charge inlet pressure grows at all engine speeds. The impacts of friction on the inlet charge are more predominant at high engine speeds with increasing heat transfer rate as the motor speed increases throughout all inlet valves. Figure 5 shows the effect of the variability of the input charge pressure on the heat transfer rate for different AFR values. On both AFR values, in-cylinder heat transfer increases as intake charge pressure grows. The effect of engine load and AFR, as well as infusion charged requirements (temperature and pressure), on the in-heat transfer characteristics was examined and accurately measured for piston insertion H2ICE. However, switching from reaction conditions to thin limits leads to a reduction in the increment pattern. The thermal conductivity has improved with rising engine speed due to increased main driver (forced convection) with energy transfer inside the cylinder. Steadily increasing AFR lowers the energy content of the hydraulic cylinder air intake charge, thus declining AFR raises the energy density of the crank shaft air intake charge. The heat transfer coefficient from either the container to the atmosphere was reported to be greater in the category of fuel cells.

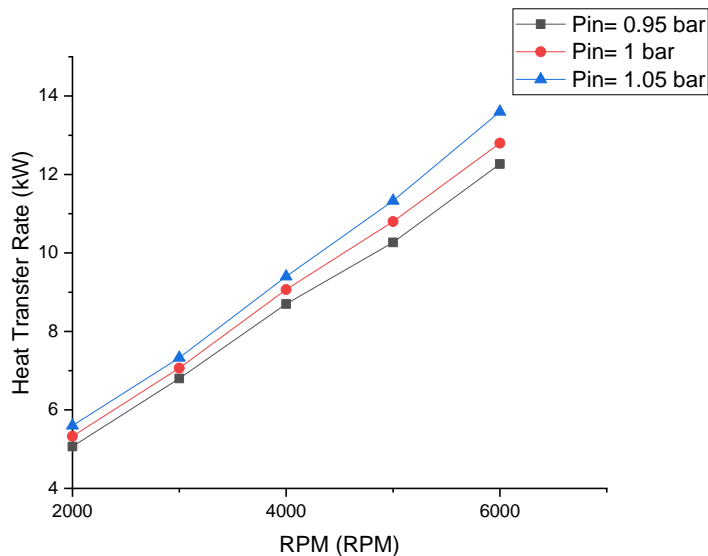


**Figure 4:** Differences in the frequency of in-cylinder heat transfer in terms of flow rate & intake charging strength.

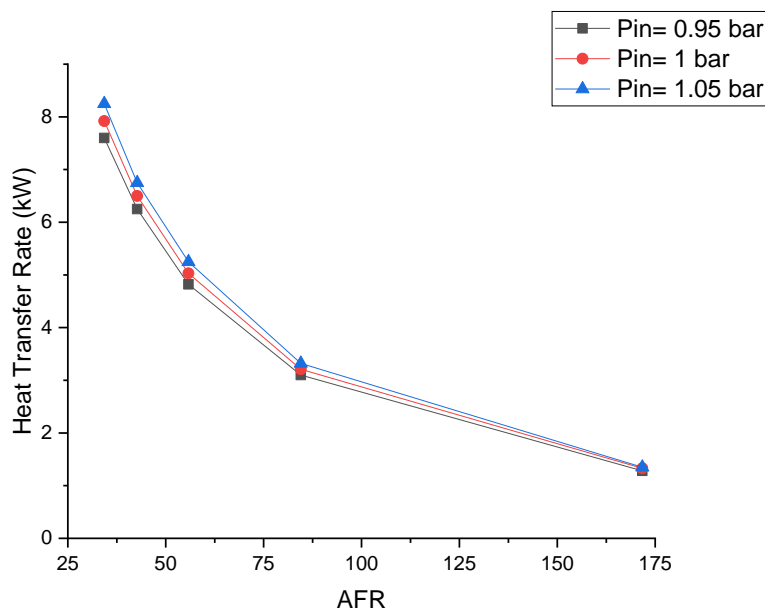


**Figure 5:** With AFR and adjustable input determine future, the in-cylinder heat transfer varies

**Thermal Conductivity and the Intensity of the Inlet Air**

Figure 6 depicts the in-cylinder heat exchange rate as a function of flow rate for various intake fuel concentrations. The in-cylinder thermal conductivity seemed to be unaffected by the injection charge temperature, especially at low rotational speed. Figure 7 depicts the cumulative effect of AFR as well as input charge temperature via the in-heat transfer rate. The voltage of the intake charge has no impact on the performance of the in-cylinder heat transfer rate even as AFR differs.

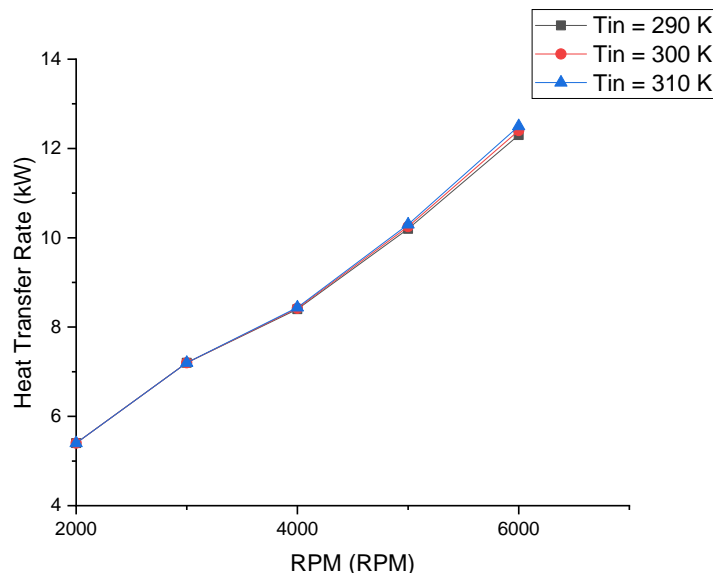


**Figure 6:** Modification inside the frequency of in-cylinder heat exchange in terms of rotational speed & input charge temperature.

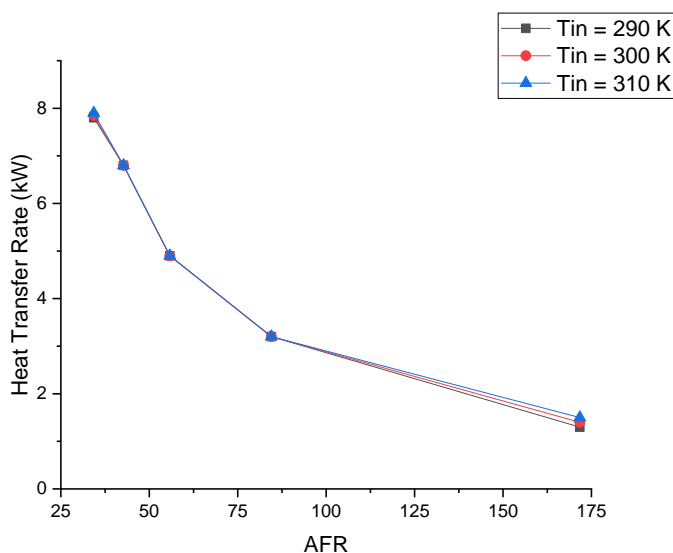


**Figure 7:** With AFR and adjustable input charge temperature, the in-cylinder temperature distribution varies.

### CONCLUSION

The effects on heat transmission features of the engine load and AFR as well as the demands for infusion loading (temperature and pressure) were examined and precision measured for H2ICE piston insertion. According to the results of the tests, increasing the input charge pressure has a serious effect on the in-cylinder heat transfer rate as engine speed but rather AFR differ. The speed of the motor was changed in 1000-rpm increments from 2100 to 5000 rpm, and the AFR was changed from particle surface to light limit. The inlet pressure was varied in 0.05-bar increments between 0.95 and 1.05 bar, and the temperature range was ranged in 10-degree increments between 270 and 320. If the AFR changes, the temperature of the intake charge does not affect the heat transfer rate for the in-cylinder, and when the engine speed changes it has a minor effect. Intake pressure variations have a higher effect than temperature variations on heat transfer characteristics, according to the results. This was also revealed why changing the intake charge pressure had little effect on lean mixtures. Furthermore, the obtained results are supported by an examination of an in-heat transfer rate's relationship with flow rate and AFR.

## REFERENCES

1. Jinesh Kumar Jain, "Optimization of Speed and Feed Rate for a Low Vibration and Better Surface Finish in Mild steel on Lathe", *International Journal of Engineering and Computer Research*, 1(3), pp. 178-184, 2012.
2. Singh, P. K., Sharma, V. K., & Islam, A. (2021). Numerical analysis on thermal properties of aluminium alloy for transforming heat based applications. *Materials Today: Proceedings*, 45, 3596-3600.
3. Eichlseder, H. Wallner, T. Freymann, R. and Ringler, J. 2003. The potential of hydrogen internal combustion engines in a future mobility scenario. SAE, Paper No 2003012267.
4. Ganesh, R. H. Subramanian, V. Balasubramanian, V. Mallikarjuna, J.M. Ramesh, A. and Sharma, R.P., 2008, Hydrogen fueled spark ignition engine with electronically controlled manifold injection: An experimental study, *Renewable Energy* 33(6), 1324–1333.
5. Kumar, A., Sharma, K., & Dixit, A. R. (2021). A review on the mechanical properties of polymer composites reinforced by carbon nanotubes and graphene. *Carbon Letters*, 31(2), 149-165.
6. Huang Z., Liu B., Zeng K., eng, Huang Y., Jiang D., Wang X., and Miao H., 2006, Experimental Study on Engine Performance and Emissions for an Engine Fueled with Natural Gas-Hydrogen Mixtures, *Energy & Fuels*, (20), 2131-2136.
7. Kahraman, E. Ozcanli, C. and Ozerdem, B. 2007. An experimental study on performance and emission characteristics of a hydrogen fuelled spark ignition engine. *Int. J. of Hydrogen Energy*, 32(12): p. 2066–2072.
8. Kim, Y.Y. Lee, J.T. and Choi, G.H. 2005. An investigation on the cause of cycle variation in direct injection hydrogen fueled engines. *Int. J. of Hydrogen Energy*, 30(1): 69-76.
9. Shukla, M. K., & Sharma, K. (2019). Effect of functionalized graphene/CNT ratio on the synergetic enhancement of mechanical and thermal properties of epoxy hybrid composite. *Materials Research Express*, 6(8), 085318.
10. Rahman, M.M., Mohammed, M.K. and Bakar, R. A., 2009, Effects of engine speed on injection timing and engine performance for 4-cylinder direct injection hydrogen fueled engine, *Canadian Journal of Pure and Applied Sciences*, (3), 731-739.
11. Saravanan N., G. Nagarajan, C. Dhanasekaran, K.M. Kalaiselvan, 2007, Experimental investigation of hydrogen port fuel injection in DI diesel engine, *Int. J. of Hydrogen Energy* (32): 4071-4080.
12. Soares, S. M. C. and Sodre, J. R. 2002. Effects of atmospheric temperature and pressure on the performance of a vehicle, *Proc Instn. Mech. Engrs. Vol. 216 Part D: J Automobile Engineering*, 216(6): 473-477.
13. Sodre, J. R. and Soares, S. M. C. 2003. Comparison of Engine Power Correction Factors for Varying Atmospheric Conditions. *J. Braz. Soc. Mech. Sci. & Eng.* 25(3):279- 284.
14. Stockhausen, W.F. Natkin, R.J. Kabat, D.M. Reams, L. Tang, X. Hashemi, S. Szwabowski S.J. and Zanardelli, V.P. 2002. Ford P2000 Hydrogen Engine Design and Vehicle Development Program. SAE, Paper No.2002-01-0240.
15. Woschni, G. 1967. A Universally Applicable Equation for the Instantaneous Heat Transfer Coefficient in the Internal Combustion Engine. SAE Paper No. 670931.